

Efficient depletion of ribosomal RNA for RNA sequencing in planarians

Iana V. Kim^{1,*}, Eric J. Ross^{2,3}, Sascha Dietrich⁴, Kristina Döring⁴, Alejandro Sánchez Alvarado^{2,3} and Claus-D. Kuhn^{1,*}

¹ Gene regulation by Non-coding RNA, Elite Network of Bavaria and University of Bayreuth, Universitätsstrasse 30, 95447 Bayreuth, Germany

² Stowers Institute for Medical Research, 1000 East 50th Street, Kansas City, MO 64110, USA

³ Howard Hughes Medical Institute, Stowers Institute for Medical Research, 1000 East 50th Street, Kansas City MO, 64110, USA

⁴ Core Unit Systems Medicine, Institute for Molecular Infection Biology, University of Würzburg, Josef-Schneider-Str. 2, 97080, Würzburg, Germany

* Corresponding authors: iana.kim@uni-bayreuth.de, claus.kuhn@uni-bayreuth.de

Abstract (350 words)

Background

The astounding regenerative abilities of planarian flatworms prompt a steadily growing interest in examining their molecular foundation. Planarian regeneration was found to require hundreds of genes and is hence a complex process. Thus, RNA interference followed by transcriptome-wide gene expression analysis by RNA-seq is a popular technique to study the impact of any particular planarian gene on regeneration. Typically, the removal of ribosomal RNA (rRNA) is the first step of all RNA-Seq library preparation protocols. To date, rRNA removal in planarians was

24 primarily achieved by the enrichment of polyadenylated (poly(A)) transcripts. However, to better
25 reflect transcriptome dynamics and to cover also non-poly(A) transcripts, a procedure for the targeted
26 removal of rRNA in planarians is needed.

27

28 **Results**

29 In this study, we describe a workflow for the efficient depletion of rRNA in the planarian model
30 species *S. mediterranea*. Our protocol is based on subtractive hybridization using organism-specific
31 probes. Importantly, the designed probes also deplete rRNA of other freshwater triclad families, a fact
32 that considerably broadens the applicability of our protocol. We tested our approach on total RNA
33 isolated stem cells (termed neoblasts) of *S. mediterranea* and compared ribodepleted libraries with
34 publicly available poly(A)-enriched ones. Overall, mRNA levels after ribodepletion were consistent with
35 poly(A) libraries. However, ribodepleted libraries revealed higher transcript levels for transposable
36 elements and histone mRNAs that remained underrepresented in poly(A) libraries. As neoblasts
37 experience high transposon activity this suggests that ribodepleted libraries better reflect the
38 transcriptional dynamics of planarian stem cells. Furthermore, the presented ribodepletion procedure
39 was successfully expanded to the removal of ribosomal RNA from the gram-negative bacterium
40 *Salmonella typhimurium*.

41

42 **Conclusions**

43 The ribodepletion protocol presented here ensures the efficient rRNA removal from low input
44 total planarian RNA, which can be further processed for RNA-Seq applications. Resulting libraries
45 contain less than 2% rRNA. Moreover, for a cost-effective and efficient removal of rRNA prior to

46 sequencing applications our procedure might be adapted to any prokaryotic or eukaryotic species of
47 choice.

48

49

50 **Keywords**

51 Planarians, Schmidtea mediterranea, ribosomal RNA removal, rRNA depletion, RNA sequencing

52

53

54

55

56

57

58

59

60

61

62

63

64

65

66

67

68

69 **Background**

70 Freshwater planarians of the species *Schmidtea mediterranea* are well known for their
71 extraordinary ability to regenerate. This ability is supported by the presence of a large population of
72 adult pluripotent stem cells, termed neoblasts [1]. Neoblasts are capable of producing all planarian
73 cell types [2]. Moreover, they preserve their potency over the whole lifespan of the animal, which
74 seems to be infinite [3]. Therefore, planarians embody an excellent model to study regeneration,
75 aging and stem cell-based diseases. The phylum Platyhelminthes, to which *S. mediterranea* belongs
76 to, includes multiple other members showing varying degrees of regenerative abilities. While some
77 freshwater species (e.g. *Dugesia japonica* and *Polycelis nigra*) are capable to restore their body from
78 any tiny piece [4, 5], others (*Procotyla fluviatilis*) have limited anterior regeneration abilities [6].
79 Altogether, the ability to regenerate is not solely based on the presence of pluripotent stem cells, but
80 represents a complex interplay between different signaling pathways. The underlying changes in gene
81 expression therefore need to be studied using transcriptome-wide techniques like RNA sequencing.

82 For any informative RNA-seq library preparation, ribosomal RNA, comprising >80% of total
83 RNA, has to be removed. To achieve this goal two strategies can be pursued: either polyadenylated
84 (poly(A)) RNA transcripts are enriched or rRNA is removed. Both approaches have advantages and
85 limitations. On the one hand, the enrichment of poly(A) transcripts ensures better coverage of coding
86 genes compared to ribodepleted samples, when sequenced to similar depth [7]. However, this
87 advantage is outweighed by the loss of transcripts lacking poly(A) tails, which include preprocessed
88 RNAs, a large share of all non-coding RNAs, such as enhancer RNAs and other long non-coding RNAs.
89 In addition, long terminal repeat (LTR) retrotransposons and various intermediates of endonucleotic
90 RNA degradation are lost during poly(A) selection [8–13]. Furthermore, most prokaryotic RNAs lack
91 poly(A) tails, making rRNA depletion crucial for the study of bacterial transcriptome [14].

92 Here, we describe a probe-based subtractive hybridization workflow for rRNA depletion that
93 efficiently removes planarian rRNA from total RNA. The protocol can be applied to input as low as 100
94 ng total RNA, which corresponds to 100,000 FACS-sorted planarian stem cells (X1 population) [15, 16].
95 Moreover, the DNA probes developed for *S. mediterranea* were successfully used for the removal of
96 ribosomal RNA in related planarian species of the order Tricladida. The rRNA removal workflow
97 presented here is also easily adapted to other organisms, as demonstrated by the removal of rRNA
98 from *Salmonella typhimurium* total RNA using organism-specific probes.

99

100

101

102

103

104

105

106

107

108

109

110

111

112

113

114

115 **Results**

116

117 **Development of an efficient rRNA depletion protocol for planarians**

118 To deplete ribosomal RNA from planarian total RNA, we chose to develop a protocol based on
119 the hybridization of rRNA-specific biotinylated DNA probes to ribosomal RNA and the capture of the
120 resulting biotinylated rRNA-DNA hybrids by use of streptavidin-coated magnetic beads (Figure 1A). To
121 that end, we synthesized a pool of 88 3'-biotinylated 40-nt long DNA oligonucleotide probes (siTOOLS
122 Biotech, Martinsried, Germany). We chose probes with a length of 40 nucleotides since their melting
123 temperature in RNA-DNA hybrids was shown to be 80 ± 6.4 °C in the presence of 500 mM sodium ions
124 [17]. This would allow probe annealing at 68°C in agreement with general probe hybridization
125 temperatures [18]. The probes were devised in antisense orientation to the following planarian rRNA
126 species: 28S, 18S type I and type II, 16S, 12S, 5S, 5.8S, internal transcribed spacer (ITS) 1 and ITS 2
127 (Supplementary Table1).

128 To assess RNA quality and the efficiency of rRNA removal we used capillary electrophoresis
129 (Fragment Analyzer, Agilent). The separation profile of total planarian RNA only shows a single rRNA
130 peak at about 1500 nucleotides (nts) (Figure 1B). This single rRNA peak is the result of the 28S rRNA
131 being processed into two fragments that co-migrate with the peak for 18S rRNA [19]. Planarian 28S
132 rRNA processing usually entails the removal of a short sequence located in the D7a expansion
133 segment of 28S rRNA. The length of the removed fragment thereby varies from 4 nts to 350 nts
134 between species (e.g. for *Dugesia japonica* 42 nts are removed) [19]. Intriguingly, a similar rRNA
135 maturation process was observed in particular protostomes, in insects such as *D. melanogaster* and in
136 other platyhelminthes [19–21]. In addition to this 28S rRNA maturation phenomenon, *S. mediterranea*

137 possesses two 18S rDNA copies that differ in about 8% of their sequence. However, only 18S rRNA
138 type I was reported to be functional and predominantly transcribed [22, 23].

139 As a first step during rRNA removal all 88 DNA probes were annealed to total planarian RNA.
140 Since RNA molecules are negatively charged, the presence of cations facilitates the annealing of
141 probes to RNA by reducing the repulsion of phosphate groups [24, 25]. Although Mg^{2+} ions are most
142 effective in stabilizing the tertiary structure of RNA and in promoting the formation of DNA-RNA
143 hybrids, they are also cofactors for multiple RNases [26] and hence should not be included during
144 ribodepletion. Therefore, we tested several hybridization buffers with varying concentrations of
145 sodium ions (Figure 1C). In the absence of sodium ions we only accomplished the incomplete removal
146 of rRNA. However, sodium concentrations >250 mM in the hybridization buffer led to the complete
147 depletion of rRNA from planarian total RNA (Figure 1C, 1D). Thus, optimal rRNA removal requires the
148 presence of >250 mM NaCl in the hybridization buffer. As we obtained the most consistent results in
149 the presence of 500 mM NaCl, we decided to utilize this salt concentration in our procedure (Figure
150 1D).

151

152 **Detailed rRNA depletion workflow**

153 **Required buffers:**

154 Hybridization buffer (20 mM Tris-HCl (pH 8.0), 1 M NaCl, 2 mM EDTA)

155 Solution A (100 mM NaOH, 50 mM NaCl, DEPC-treated)

156 Solution B (100 mM NaCl, DEPC-treated)

157 2xB&W (Binding&Washing) buffer (10 mM Tris-HCl (pH 7.5), 1 mM EDTA, 2 M NaCl)

158 Dilution buffer (10 mM Tris-HCl (pH 7.5), 200 mM NaCl, 1 mM EDTA)

159 **Protocol:**

160 1. RNA input

161 The following protocol efficiently depletes ribosomal RNA from 100 up to 1.5 μg of total RNA (Figure
162 1E). The procedure can be scaled up for higher RNA input.

163 2. Hybridization of biotinylated DNA oligonucleotides (40-mers) to ribosomal RNA.

164 a) For oligonucleotide annealing the following reaction is set up:

165 10 μl hybridization buffer

166 10 μl RNA input (1 μg)

167 1 μl 100 μM biotinylated DNA 40-mers probes

168 b) Gently mix the solution by pipetting and incubate at 68 $^{\circ}\text{C}$ for 10 min.

169 c) Immediately transfer the tubes to 37 $^{\circ}\text{C}$ for 30 min.

170 3. Prepare Dynabeads MyOne Streptavidin C1 (Invitrogen) according to the manufacturer's instruction
171 as follows:

172 a) For each sample use 120 μl (10 $\mu\text{g}/\mu\text{l}$) of beads slurry.

173 b) Wash the beads twice with an equal volume (or at least 1 ml) of Solution A. Add Solution A and
174 incubate the mixture for 2 min. Then, place the tube on a magnet for 1 min and discard the
175 supernatant.

176 c) Wash the beads once in Solution B. Split the washed beads into two separate tubes for two
177 rounds of subtractive rRNA depletion (Round1 and Round2). Place the beads on a magnet for 1
178 min and discard Solution B.

179 d) Resuspend the Round1 beads in 2xB&W buffer to a final concentration of 5 $\mu\text{g}/\mu\text{l}$ (twice the
180 original volume). The Round1 beads will be used during the first round of rRNA depletion. For the
181 second round of depletion, resuspend the Round2 beads to a final concentration of 5 $\mu\text{g}/\mu\text{l}$ in

182 1xB&W buffer. The Round2 beads will be used in a second depletion step. Keep it at 37 °C until
183 required.

184 4. Capture of DNA-RNA hybrids using magnetic beads (step 2).

185 a) Briefly spin down the tubes containing total RNA and probes. Add the following:

186 100 µl dilution buffer

187 120 µl washed magnetic beads (5 µg/µl) in 2xB&W (Round1).

188 Resuspend by pipetting up and down ten times. The final concentration of NaCl during this step is
189 1 M. Incubate the solution at 37 °C for 15 min. Gently mix the sample occasionally by tapping.

190 b) Place on magnet for 2 min. Carefully remove the supernatant and add the additional 120 µl of
191 washed magnetic beads in 1xB&W (Round2). Incubate the mixture at 37°C for 15 min with
192 occasional gentle tapping.

193 c) Place on magnet for 2 min. Carefully transfer the supernatant into a new tube and place it on
194 magnet for another 1 min to remove all traces of magnetic beads from the sample.

195 d) Transfer the supernatant into a fresh tube.

196 5. Use the RNA Clean & Concentrator-5 kit (Zymo Research) to concentrate the ribodepleted samples,
197 to carry out size selection and to digest any remaining DNA using DNase I treatment as described [27].

198

199 **Ribosomal RNA depletion in planarian species related to *S. mediterranea***

200 Ribosomal DNA genes are among the most conserved sequences in the kingdom of life. They
201 are present in all organisms and are widely used for the construction of phylogenetic trees [28]. The
202 latter is possible because of the low rate of nucleotide substitutions in rRNA sequences (about 1 - 2%
203 substitutions occur per 50 million years based on bacterial 16S rRNA) [29]. The divergence of 18S
204 rRNA sequence between different families of freshwater planarians lays in the range of 6 – 8%, while

205 interspecies diversity does not exceed 4% [23]. Therefore, low rRNA divergence between taxa can be
206 exploited for the design of universal probes for rRNA depletion in different organisms. To assess the
207 specificity and universal applicability of our DNA probes, we depleted rRNA in flatworm species of the
208 order Tricladida, all related to *S. mediterranea* (Figure 2A). Total RNA separation profiles were
209 analyzed before and after rRNA depletion of six planarian species from three different families. Two
210 of these, *Dugesia japonica* and *Cura pinguis* belong to the same family as *S. mediterranea*, the
211 Dugesiiidae family. In addition, we examined three species from the family Planariidae (*Planaria torva*,
212 *Polycelis nigra* and *Polycelis tenuis*) and one species from the genus *Camerata* of Uteriporidae
213 (subfamily Uteriporinae). For all tested species our DNA probes proved efficient for the complete
214 removal of rRNA, which migrated close to 2000 nts on all electropherograms (Figure 2B). Thus, the
215 probes presented here can be utilized for the removal of ribosomal RNA in a multitude of planarian
216 species and may even be generally applicable to all studied planarian species.

217

218 **Comparison of RNA-Seq libraries prepared by ribodepletion or poly(A) selection**

219 To assess the efficiency of rRNA removal and the specificity of our DNA probes, we prepared
220 and analyzed RNA-Seq libraries from ribodepleted planarian total RNA from *S. mediterranea*. Total
221 RNA was extracted from 100,000 FACS-sorted planarian neoblasts, resulting in 70 – 100 ng of input
222 RNA. RNA-Seq libraries were prepared and sequenced as described [27] following 15 cycles of PCR
223 amplification. The subsequent analysis of sequenced libraries confirmed the efficient removal of
224 rRNAs. Less than 2% of total sequenced reads constituted ribosomal RNA (Figure 3A). Next, we
225 compared our rRNA-depleted libraries with three publicly available planarian poly(A) enriched RNA-
226 Seq datasets (poly(A) libraries) [30–32]. In case publicly available libraries were sequenced in paired-
227 end mode, we analyzed only the first read of every pair to minimize the technical variation between

228 libraries [33]. As shown in Figure 3A, the ribodepleted libraries contained significantly less rRNA
229 compared to all poly(A) enriched ones. Interestingly, the major rRNA species that remained after
230 poly(A) selection was mitochondrial 16S rRNA (Figure 3B). Although the planarian genome has a high
231 A-T content (> 70%) [34], we could not attribute the overrepresentation of 16S rRNA in poly(A)
232 libraries to a high frequency or longer stretches of A nucleotides as compared to other rRNA species
233 (Figure 3C). Moreover, using publicly available planarian poly(A)-position profiling by sequencing (3P-
234 Seq) libraries [35] which allow the identification of 3'-ends of polyadenylated RNAs, no
235 polyadenylation sites were detected on 16S rRNA. Therefore, we speculate that upon folding of the
236 16S rRNA stretches of A nucleotides become exposed and facilitate the interaction with oligo-dT
237 beads during transcript poly(A) selection.

238 We next assigned the analyzed datasets to the planarian genome. In ribodepleted libraries
239 more than 13% of all mapped reads were assigned to intergenic regions, compared to 7% – 10.5% for
240 poly(A)-enriched ones (Figure 3D). In addition, the percentage of unmapped reads was higher in
241 ribodepleted libraries and constituted about 17.6%, which is on average 2.4% more than in poly(A)
242 datasets. We speculate that for ribodepleted libraries the proportion of reads mapping to intergenic
243 regions will increase in future once complete assemblies of the planarian genome are available.
244 Currently, the planarian genome assembly consists of 481 scaffolds [34]. To detect gene expression
245 variabilities between the analyzed libraries, we performed principal component analysis for the
246 clustering of gene expression data. Although all poly(A) selected libraries were grouped closer
247 together along the PC1 scale, all four analyzed datasets appeared as separated clusters. This indicates
248 the presence of considerable variation even amongst different batches of poly(A) libraries (Figures
249 3E). One possible source of such variation might be the sequencing depth of the analyzed libraries,
250 which varied considerably from 13 to 64 million of mapped reads (Figure 3F).

251 Next, to estimate the correlation between ribodepleted and poly(A) libraries, we calculated
252 their Pearson correlation coefficients (Figure 3G). We found the highest Pearson correlation between
253 ribodepleted libraries and polyA B2 samples ($R=0.94$, $p < 2.2e-16$) (Figure 3F). This could be due to
254 their similar sequencing depth compared to the other polyA libraries. The transcripts whose
255 abundance was most significantly affected by poly(A) selection were found to be histone mRNAs that
256 are known to lack polyA tails (Figure 3G, 3H) [36]. Their expression level appeared to be 8 – 10 fold
257 higher in our ribodepleted libraries. Moreover, in the ribodepleted libraries we detected significantly
258 higher expression levels for transposable elements (Figure 3G, 3I). Out of 316 planarian transposable
259 element families [37] 254 were on average upregulated 5.2, 3.5 and 4.0 fold as compared to polyA B1,
260 polyA B2 and polyA B3 libraries, respectively (Figure 3I). Our ribodepleted libraries revealed that Burro
261 elements, giant retroelements found in planarian genome [34], gypsy retrotransposons, hAT and
262 Mariner/Tc1 DNA transposons are the most active transposable elements in planarian stem cells.
263 Although some of transposable elements are polyadenylated, long-terminal repeat elements (LTRs)
264 lack poly(A)-tails [38]. This renders their detection in poly(A)-enriched sample non-quantitative. Last,
265 our rRNA depletion workflow also allows for the detection of transposable element degradation
266 products that were generated by PIWI proteins guided by specific piRNAs, an abundant class of small
267 RNAs in planarians [39, 40].

268

269 **Non-specific depletion of coding transcripts in ribodepleted libraries**

270 In using custom ribodepletion probes, our major concern was that the utilized probes would
271 lead to unspecific co-depletion of planarian coding transcripts. To exclude this possibility, we first
272 mapped our pool of 88 DNA probes in antisense orientation to the planarian transcriptome allowing
273 up to 8 mismatches and gaps of up to 3 nts. This mapping strategy requires at least 75% of a DNA

274 probe to anneal to its RNA target. It resulted in only 11 planarian genes to be potentially recognized
275 by 20 DNA probes from our oligonucleotide pool. Next, we carried out a differential expression
276 analysis of these 11 potentially targeted transcripts between the ribodepleted libraries and poly(A)-
277 selected ones. The analysis revealed that 9 out of 11 potential targets were downregulated at least 1-
278 fold in at least two poly(A) experiments (Figure 4A). As the abundance of three transcripts
279 (SMESG000014330.1 (rhodopsin-like orphan gpcr [41]), SMESG000068163.1 and SMESG000069530.1
280 (both without annotation)) was very low in all polyA libraries (<0.6 transcripts per million (TPM)) we
281 did not consider these any further. However, we found the remaining six transcripts to be significantly
282 downregulated in ribodepleted libraries. For three of these targeted genes (SMESG000067473.1,
283 SMESG000021061.1 and SMESG000044545.1) the probes map in regions that display significant RNA-
284 seq coverage (Figure 4B, Supplemental Figs. S1A, S1B). Therefore, their lower expression values in
285 ribodepleted libraries is likely attributed to probe targeting. Intriguingly, for the remaining three
286 targets (SMESG000066644.1, SMESG000043656.1 and SMESG000022863.1 annotated as RPL26
287 (ribosomal protein L26), COX11 (cytochrome c oxidase copper chaperone) and an unknown transcript,
288 respectively) the probes were predicted to map to loci that do not exhibit RNA-seq coverage (Figure
289 4C, Supplemental Figs. S1C, S1D). The likely reason for this is inaccurate gene annotation.
290 Alternatively, target regions might represent repetitive, multimapping sequences, which we excluded
291 during read mapping. Taken together, our off-target analysis revealed that a maximum of 11 genes
292 might be affected by our rRNA removal procedure - a very low number that underscores the
293 specificity and efficiency of our depletion protocol.

294
295 **Applicability of the described ribodepletion method to other organisms**

296 To demonstrate the applicability of the developed rRNA workflow to other organisms, we
297 employed our protocol to the depletion of ribosomal RNA from *Salmonella typhimurium* using a pool
298 of organism-specific DNA probes (riboPOOL) developed by siTOOLS Biotech (Martinsried, Germany)
299 (Figure 5A). We compared the libraries resulting from the application of our newly developed
300 procedure to the established rRNA depletion workflow that utilizes the Ribo-Zero rRNA Removal Kit
301 (Bacteria) from Illumina. Removal of rRNA from a *S. typhimurium* sample using riboPOOL probes was
302 comparably successful as a depletion reaction using Ribo-Zero, leaving as low as 3.4% rRNA in the final
303 library (Figure 5A). Moreover, an overall comparison of gene expression levels showed a high
304 correlation (Pearson correlation > 0.98) between riboPOOL depleted libraries and libraries prepared
305 with the Ribo-Zero kit (Figure 5B). Taken together, the rRNA depletion workflow described in this
306 manuscript is robust and easily applicable to any bacterial and eukaryotic species of choice utilizing
307 organism-specific probes.

308

309 Discussion

310 For samples from typical model organisms, such as human, mouse and rat, there are
311 numerous commercial kits available for the removal of rRNA, e.g. NEBNext from New England Biolabs,
312 RiboGone from Takara and RiboCop from Lexogen. This also applies to typical gram-positive and
313 gram-negative bacteria (MICROBExpress from Thermofisher and Ribominus from Invitrogen).
314 Moreover, these kits can be utilized with a certain degree of compatibility for the depletion of rRNA in
315 organisms of distant phylogenetic groups (e.g. RiboMinus Eukaryote Kit for RNA-Seq, Invitrogen).
316 However, as the breadth of molecularly tractable organisms increases in the past decade, the
317 necessity to develop organism-specific rRNA depletion techniques rises as well [42–44]. To date, such
318 custom protocols were either based on rRNA removal by biotinylated antisense probes along with

319 streptavidin-coated magnetic beads or they were based on the digestion of DNA-RNA hybrids with
320 RNase H [14, 45–47].

321 In this study, we describe a novel rRNA depletion workflow for the planarian flatworm *S.*
322 *mediterranea*. Our protocol is based on the hybridization of biotinylated DNA probes to planarian
323 rRNA followed by the subsequent removal of the resulting rRNA-DNA hybrids with streptavidin-
324 labeled magnetic beads. A comparative analysis between ribodepleted and poly(A)-selected libraries
325 in planarians revealed that our protocol retains all information present in poly(A) selected libraries.
326 Over and above, we found ribodepleted libraries to contain additional information on histone mRNAs,
327 transposable elements (of which many do not have polyA tails) and transcriptional intermediates. This
328 highlights that ribodepletion better retains the dynamic information of transcriptomes. As more and
329 more co-translational decay pathways are being discovered [48], understanding the dynamic of RNA
330 degradation will become more important in the near future. Moreover, by successfully depleting
331 rRNA from other freshwater triclad species, we could demonstrate the versatility of the DNA probes
332 designed for *S. mediterranea*. Last, we validated the efficiency of the developed workflow by removal
333 of rRNA in the gram-negative bacterium *S. typhimurium*. Therefore, the proposed workflow serves as
334 an efficient and cost-effective method for rRNA depletion in any organism of interest.

335

336 **Conclusions**

337 This study describes an rRNA depletion workflow for the planarian model system *S.*
338 *mediterranea* and related freshwater triclads. It is based on the hybridization of 40-mer biotinylated
339 DNA oligos to ribosomal RNA followed by the subtraction of formed DNA-RNA hybrids. The protocol is
340 very robust and ensures the efficient removal of rRNA even from low input total RNA. Moreover, we

341 suggest the general applicability of the presented workflow to any prokaryotic or eukaryotic
342 organisms by using organism-specific pools of probes.

343

344

345

346

347

348

349

350

351

352

353

354

355

356

357

358

359

360

361

362

363

364 **Materials and Methods**

365

366 **Ribosomal RNA depletion**

367 Ribosomal RNA depletion was conducted as described in the result section. To evaluate
368 Fragment analyzer separation profiles, planarian total RNA (1000 ng each sample) was subjected to
369 rRNA depletion using varying concentrations of NaCl (0 mM, 50 mM, 250 mM, 500 mM) in the
370 hybridization buffer.

371

372 **Phylogenetic tree**

373 The phylogenetic tree was constructed using NCBI taxonomic names at phyloT
374 (<https://phylo.t.biobyte.de>). The tree was visualized using the Interactive Tree of Life (iTOL) tool [49].

375

376 **Planarian rRNA-depleted RNA-Seq dataset**

377 Raw sequencing reads for planarian rRNA-depleted dataset were downloaded from the project
378 GSE122199 (GSM3460490, GSM3460491, GSM3460492). The libraries were prepared as described
379 [40]. Briefly, planarian rRNA depleted RNA-Seq libraries were prepared from 100,000 FACS-sorted
380 planarian X1 cells as described [27] and sequenced on an Illumina Next-Seq 500 platform (single-end,
381 75 bp).

382

383 **Publicly available RNA-Seq datasets**

384 Raw sequencing reads for all datasets were downloaded from the Sequence read archive
385 (SRA). Planarian polyA B1 rep1, polyA B1 rep2, polyA B1 rep3 correspond to SRR2407875,
386 SRR2407876, and SRR2407877, respectively, from the Bioproject PRJNA296017 (GEO: GSE73027) [30].

387 Planarian polyA B2 rep1, polyA B2 rep2 samples correspond to SRR4068859, SRR4068860 from the
388 Bioproject PRJNA338115 [32]. Planarian polyA B3 rep1, polyA B3 rep2, polyA B3 rep3 correspond to
389 SRR7070906, SRR7070907, SRR7070908, respectively, (PRJNA397855) [31]. Only first read of the pair
390 was analyzed for polyA B2 and polyA B3 from Bioprojects PRJNA338115 and PRJNA397855.

391

392 ***Salmonella typhimurium* SL1344 RNA Seq datasets**

393 In total, four samples were sequenced for *Salmonella typhimurium* SL1344 by the IMGM
394 Laboratories GmbH (Martinsried, Germany) on an Illumina NextSeq 500 platform (single-end, 75bp).
395 Of these sequenced samples, one sample was of untreated total RNA, two samples were of RiboZero
396 and one of RiboPools treated total RNA. The sequencing data are available at NCBI Gene Expression
397 Omnibus (<http://www.ncbi.nlm.nih.gov/geo>) under the accession number GSE132630.

398

399 **Processing of RNA-Seq libraries**

400 Planarian RNA-Seq data were processed as follows: Reads after removal of 3'-adapters and
401 quality filtering with Trimmomatic (0.36) [50] were trimmed to a length of 50 nt. For libraries
402 sequenced in pair-end mode, only the first read of a pair was considered for the analysis. Next,
403 sequences mapped to planarian rRNAs were removed with SortMeRNA [51]. Reads were assigned to
404 the reference genome version SMESG.1 [34] or consensus transposable element sequences [37] in
405 strand-specific mode and quantified with Kallisto [52] with "--single -l 350 -s 30 -b 30". Differential
406 gene expression analysis was performed with DeSeq2 [53]. To annotate RNA-Seq reads to coding
407 regions (CDS), reads were mapped to the planarian genome using STAR [54] with the following
408 setting: --quantMode TranscriptomeSam --outFilterMultimapNmax 1.

409 RNA sequencing data from *Salmonella typhimurium* SL1344 were processed with
410 READemption 0.4.3 using default parameters [55]. Sequenced reads were mapped to the RefSeq
411 genome version NC_016810.1 and plasmids NC_017718.1, NC_017719.1, NC_017720.1.

412

413 **Analysis of DNA probe specificity**

414 DNA probe sequences were mapped to the planarian transcriptome SMEST.1 [56] using the
415 BURST aligner (v0.99.7LL; DB15) [57] with the following settings “-fr -i .80 -m FORAGE”. Only
416 sequences that mapped to genes in antisense orientation with no more than 8 mismatches were
417 considered as potential probe targets.

418

419

420 **Acknowledgements**

421 We thank Jochen Rink, Mario Ivankovic and Miquel Vila Farré from the Max Planck Institute of
422 Molecular Cell Biology and Genetics in Dresden for generously providing various flatworm species. We
423 thank Jens Hör from the Institute for Molecular Infection Biology, University of Würzburg, for
424 providing the *Salmonella* RNA and IMGM Laboratories for library preparation and sequencing of
425 *Salmonella* samples. We also acknowledge the KeyLab Genomics & Bioinformatics at the University of
426 Bayreuth for Fragment Analyzer (Agilent) measurements. This work was supported by the Elite
427 Network of Bavaria, the University of Bayreuth, the Paul Ehrlich and Ludwig Darmstaedter Prize for
428 Young Researchers (to C.D.K) and the IZKF at the University of Würzburg (project Z-6). A.S.A. is an
429 investigator of the Howard Hughes Medical Institute and the Stowers Institute for Medical Research.

430

431 **Competing interests**

432 The authors declare that they have no competing interests.

433

434 **Authors' contributions**

435 I.V.K. and C.D.K. conceived and designed the study; I.V.K. and K.D. acquired data; E.J.R.
436 assembled planarian rRNA sequences; I.V.K., E.J.R. and S.D. performed computation analyses; A.S.A.
437 and C.D.K. supervised the study; I.V.K. and C.D.K. drafted the manuscript with input from all authors.

438 **References**

- 439 1. Elliott SA, Sánchez Alvarado A. The history and enduring contributions of planarians to the study of
440 animal regeneration. *Wiley Interdiscip Rev Dev Biol.* 2013;2:301–26. doi:10.1002/wdev.82.
- 441 2. Zeng A, Li H, Guo L, Gao X, McKinney S, Wang Y, et al. Prospectively isolated tetraspanin+ neoblasts
442 are adult pluripotent stem cells underlying planaria regeneration. *Cell.* 2018;173:1593–608.
- 443 3. Sahu S, Dattani A, Aboobaker AA. Secrets from immortal worms: What can we learn about
444 biological ageing from the planarian model system? *Semin Cell Dev Biol.* 2017;70:108–21.
445 doi:10.1016/j.semcd.2017.08.028.
- 446 4. Collins JJ. Platyhelminthes. *Curr Biol.* 2017;27:R252–6. doi:10.1016/J.CUB.2017.02.016.
- 447 5. Egger B, Gschwentner R, Rieger R. Free-living flatworms under the knife: past and present. *Dev*
448 *Genes Evol.* 2007;217:89–104. doi:10.1007/s00427-006-0120-5.
- 449 6. Sikes JM, Newmark PA. Restoration of anterior regeneration in a planarian with limited
450 regenerative ability. *Nature.* 2013;500:77–80. doi:10.1038/nature12403.
- 451 7. Zhao W, He X, Hoadley KA, Parker JS, Hayes D, Perou CM. Comparison of RNA-Seq by poly (A)
452 capture, ribosomal RNA depletion, and DNA microarray for expression profiling. *BMC Genomics.*
453 2014;15:419. doi:10.1186/1471-2164-15-419.
- 454 8. Katayama S, Tomaru Y, Kasukawa T, Waki K, Nakanishi M, Nakamura M, et al. Antisense
455 transcription in the mammalian transcriptome. *Science.* 2005;309:1564–6.
456 doi:10.1126/science.1112009.
- 457 9. Cheng J, Kapranov P, Drenkow J, Dike S, Brubaker S, Patel S, et al. Transcriptional Maps of 10

- 458 Human Chromosomes at 5-Nucleotide Resolution. *Science* (80-). 2005;308:1149–54.
459 doi:10.1126/SCIENCE.1108625.
- 460 10. Kim T-K, Hemberg M, Gray JM, Costa AM, Bear DM, Wu J, et al. Widespread transcription at
461 neuronal activity-regulated enhancers. *Nature*. 2010;465:182. doi:10.1038/NATURE09033.
- 462 11. Finnegan DJ. Retrotransposons. *Curr Biol*. 2012;22:R432–7. doi:10.1016/J.CUB.2012.04.025.
- 463 12. Reuter M, Berninger P, Chuma S, Shah H, Hosokawa M, Funaya C, et al. Miwi catalysis is required
464 for piRNA amplification-independent LINE1 transposon silencing. *Nature*. 2011;480:264–7.
465 doi:10.1038/nature10672.
- 466 13. Wang W, Yoshikawa M, Han BW, Izumi N, Tomari Y, Weng Z, et al. The initial uridine of primary
467 piRNAs does not create the tenth adenine that is the hallmark of secondary piRNAs. *Mol Cell*.
468 2014;56:708–16. doi:10.1016/j.molcel.2014.10.016.
- 469 14. Kukutla P, Steritz M, Xu J. Depletion of Ribosomal RNA for Mosquito Gut Metagenomic RNA-seq. *J*
470 *Vis Exp*. 2013. doi:10.3791/50093.
- 471 15. Reddien PW, Oviedo NJ, Jennings JR, Jenkin JC, Sánchez Alvarado A. Developmental biology:
472 SMEDWI-2 is a PIWI-like protein that regulates planarian stem cells. *Science* (80-). 2005;310:1327–30.
- 473 16. Hayashi T, Asami M, Higuchi S, Shibata N, Agata K. Isolation of planarian X-ray-sensitive stem cells
474 by fluorescence-activated cell sorting. *Dev Growth Differ*. 2006;48:371–80.
- 475 17. Wetmur JG. DNA Probes: Applications of the Principles of Nucleic Acid Hybridization. *Crit Rev*
476 *Biochem Mol Biol*. 1991;26:227–59. doi:10.3109/10409239109114069.
- 477 18. Green MR, Sambrook J. *Molecular Cloning, 3-Volume Set : A Laboratory Manual*. 2012.

- 478 19. Sun S, Xie H, Sun Y, Song J, Li Z. Molecular characterization of gap region in 28S rRNA molecules in
479 brine shrimp *Artemia parthenogenetica* and planarian *Dugesia japonica*. *Biochem.* 2012;77:411–7.
- 480 20. van Keulen H, Mertz PM, LoVerde PT, Shi H, Rekosh DM. Characterization of a 54-nucleotide gap
481 region in the 28S rRNA gene of *Schistosoma mansoni*. *Mol Biochem Parasitol.* 1991;45:205–14.
482 doi:10.1016/0166-6851(91)90087-M.
- 483 21. Ware VC, Renkawitz R, Gerbi SA. rRNA processing: removal of only nineteen bases at the gap
484 between 28S alpha and 28S beta rRNAs in *Sciara coprophila*. *Nucleic Acids Res.* 1985;13:3581–97.
485 <http://www.ncbi.nlm.nih.gov/pubmed/2989775>. Accessed 16 Apr 2019.
- 486 22. Carranza S, Bagnà J, Riutort M. Origin and Evolution of Paralogous rRNA Gene Clusters Within the
487 Flatworm Family Dugesidae (Platyhelminthes, Tricladida). *J Mol Evol.* 1999;49:250–9.
488 doi:10.1007/PL00006547.
- 489 23. Carranza S, Giribet G, Ribera C, Riutort M. Evidence that two types of 18S rDNA coexist in the
490 genome of *Dugesia (Schmidtea) mediterranea* (Platyhelminthes, Turbellaria, Tricladida). *Mol Biol Evol.*
491 1996;13:824–32. doi:10.1093/oxfordjournals.molbev.a025643.
- 492 24. Draper DE. A guide to ions and RNA structure. *RNA.* 2004;10:335–43. doi:10.1261/RNA.5205404.
- 493 25. Lambert D, Lepply D, Shiman R, Draper DE. The influence of monovalent cation size on the
494 stability of RNA tertiary structures. *J Mol Biol.* 2009;390:791–804. doi:10.1016/j.jmb.2009.04.083.
- 495 26. Garrey SM, Blech M, Riffell JL, Hankins JS, Stickney LM, Diver M, et al. Substrate binding and active
496 site residues in RNases E and G: role of the 5'-sensor. *J Biol Chem.* 2009;284:31843–50.
497 doi:10.1074/jbc.M109.063263.

- 498 27. Zhang Z, Theurkauf WE, Weng Z, Zamore PD. Strand-specific libraries for high throughput RNA
499 sequencing (RNA-Seq) prepared without poly(A) selection. *Silence*. 2012;3:9. doi:10.1186/1758-907X-
500 3-9.
- 501 28. Woese CR. Interpreting the universal phylogenetic tree. *Proc Natl Acad Sci U S A*. 2000;97:8392–6.
- 502 29. Ochman H, Elwyn S, Moran NA. Calibrating bacterial evolution. *Proc Natl Acad Sci*.
503 1999;96:12638–43.
- 504 30. Duncan EM, Chitsazan AD, Seidel CW, Alvarado AS. Erratum: Set1 and MLL1/2 Target Distinct Sets
505 of Functionally Different Genomic Loci In Vivo (*Cell Reports* (2015) 13 (12) (p2741–
506 2755)(S2211124715014084)(10.1016/j.celrep.2015.11.059)). *Cell Rep*. 2016;17:930.
- 507 31. Schmidt D, Reuter H, Hüttner K, Ruhe L, Rabert F, Seebeck F, et al. The Integrator complex
508 regulates differential snRNA processing and fate of adult stem cells in the highly regenerative
509 planarian *Schmidtea mediterranea*. *PLoS Genet*. 2018;14:e1007828.
510 doi:10.1371/journal.pgen.1007828.
- 511 32. Mihaylova Y, Abnave P, Kao D, Hughes S, Lai A, Jaber-Hijazi F, et al. Conservation of epigenetic
512 regulation by the MLL3/4 tumour suppressor in planarian pluripotent stem cells. *Nat Commun*.
513 2018;9:3633. doi:10.1038/s41467-018-06092-6.
- 514 33. Williams AG, Thomas S, Wyman SK, Holloway AK. RNA-seq Data: Challenges in and
515 Recommendations for Experimental Design and Analysis. *Curr Protoc Hum Genet*. 2014;83:11.13.1-20.
516 doi:10.1002/0471142905.hg1113s83.
- 517 34. Grohme MA, Schloissnig S, Rozanski A, Pippel M, Young GR, Winkler S, et al. The genome of

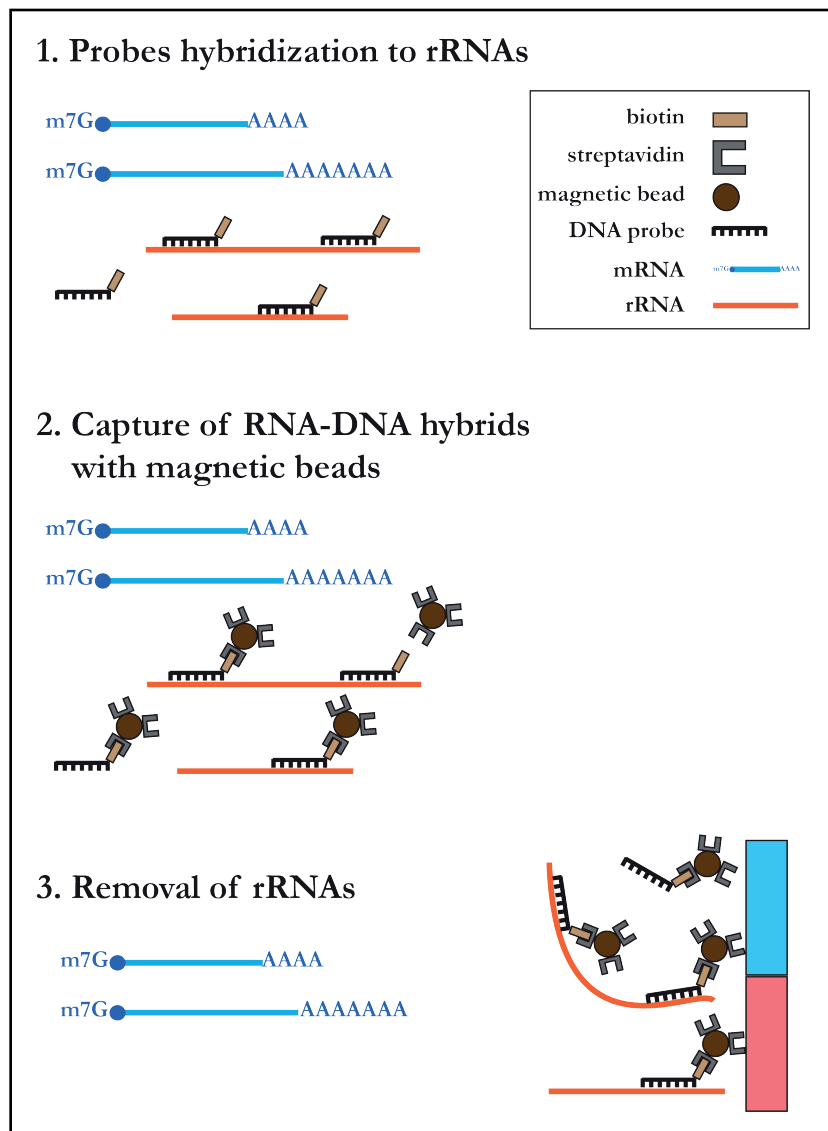
- 518 *Schmidtea mediterranea* and the evolution of core cellular mechanisms. *Nature*. 2018;554:56–61.
519 doi:10.1038/nature25473.
- 520 35. Lakshmanan V, Bansal D, Kulkarni J, Poduval D, Krishna S, Sasidharan V, et al. Genome-Wide
521 Analysis of Polyadenylation Events in *Schmidtea mediterranea*. *Genes & Genomes*.
522 *Genes | Genomes | Genetics*. 2016.
- 523 36. Marzluff WF, Wagner EJ, Duronio RJ. Metabolism and regulation of canonical histone mRNAs: Life
524 without a poly(A) tail. *Nature Reviews Genetics*. 2008;:843–54.
- 525 37. Bao W, Kojima KK, Kohany O. Repbase Update, a database of repetitive elements in eukaryotic
526 genomes. *Mob DNA*. 2015;6:11. doi:10.1186/s13100-015-0041-9.
- 527 38. Kazazian HH. Mobile Elements : Drivers of Genome Evolution. *Science (80-)*. 2004;303:1626–32.
528 doi:10.1126/science.1089670.
- 529 39. Shibata N, Kashima M, Ishiko T, Nishimura O, Rouhana L, Misaki K, et al. Inheritance of a Nuclear
530 PIWI from Pluripotent Stem Cells by Somatic Descendants Ensures Differentiation by Silencing
531 Transposons in Planarian. *Dev Cell*. 2016;37:226–37. doi:10.1016/j.devcel.2016.04.009.
- 532 40. Kim I V., Duncan EM, Ross EJ, Gorbovytska V, Nowotarski S, Elliott SA, et al. Planarians recruit
533 piRNAs for mRNA turnover in adult stem cells. In revision.
- 534 41. Saberi A, Jamal A, Beets I, Schoofs L, Newmark PA. GPCRs Direct Germline Development and
535 Somatic Gonad Function in Planarians. *PLoS Biol*. 2016;14:e1002457.
536 doi:10.1371/journal.pbio.1002457.
- 537 42. Dietrich MR, Ankeny RA, Chen PM. Publication trends in model organism research. *Genetics*.

- 538 2014;198:787–94. doi:10.1534/genetics.114.169714.
- 539 43. Goldstein B, King N. The Future of Cell Biology: Emerging Model Organisms. *Trends Cell Biol.*
540 2016;26:818–24. doi:10.1016/j.tcb.2016.08.005.
- 541 44. Russell JJ, Theriot JA, Sood P, Marshall WF, Landweber LF, Fritz-Laylin L, et al. Non-model model
542 organisms. *BMC Biol.* 2017;15:55. doi:10.1186/s12915-017-0391-5.
- 543 45. O’Neil D, Glowatz H, Schlumpberger M. Ribosomal RNA Depletion for Efficient Use of RNA-Seq
544 Capacity. In: *Current Protocols in Molecular Biology*. Hoboken, NJ, USA: John Wiley & Sons, Inc.; 2013.
545 p. 4.19.1-4.19.8. doi:10.1002/0471142727.mb0419s103.
- 546 46. Li S-K, Zhou J-W, Yim AK-Y, Leung AK-Y, Tsui SK-W, Chan T-F, et al. Organism-specific rRNA capture
547 system for application in next-generation sequencing. *PLoS One.* 2013;8:e74286.
548 doi:10.1371/journal.pone.0074286.
- 549 47. Morlan JD, Qu K, Sinicropi D V. Selective depletion of rRNA enables whole transcriptome profiling
550 of archival fixed tissue. *PLoS One.* 2012;7:e42882. doi:10.1371/journal.pone.0042882.
- 551 48. Ibrahim F, Maragkakis M, Alexiou P, Mourelatos Z. Ribothrypsis, a novel process of canonical
552 mRNA decay, mediates ribosome-phased mRNA endonucleolysis. *Nat Struct Mol Biol.* 2018;25:302–
553 310.
- 554 49. Letunic I, Bork P. Interactive Tree Of Life (iTOL) v4: recent updates and new developments. *Nucleic
555 Acids Res.* 2019. doi:10.1093/nar/gkz239.
- 556 50. Bolger AM, Lohse M, Usadel B. Trimmomatic: a flexible trimmer for Illumina sequence data.
557 *Bioinformatics.* 2014;30:2114–20. doi:10.1093/bioinformatics/btu170.

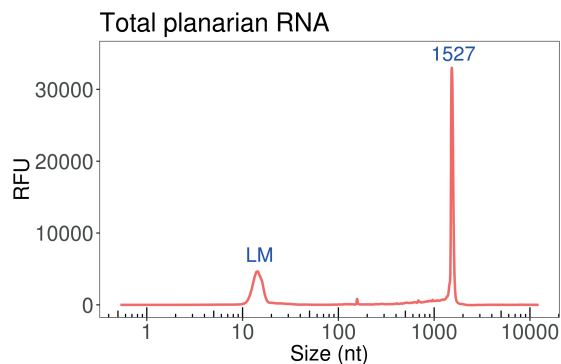
- 558 51. Kopylova E, Noé L, Touzet H. SortMeRNA: fast and accurate filtering of ribosomal RNAs in
559 metatranscriptomic data. *Bioinformatics*. 2012;28:3211–7. doi:10.1093/bioinformatics/bts611.
- 560 52. Bray NL, Pimentel H, Melsted P, Pachter L. Near-optimal probabilistic RNA-seq quantification. *Nat*
561 *Biotechnol*. 2016;34:525–7. doi:10.1038/nbt.3519.
- 562 53. Love MI, Huber W, Anders S. Moderated estimation of fold change and dispersion for RNA-seq
563 data with DESeq2. *Genome Biol*. 2014;15:550. doi:10.1186/s13059-014-0550-8.
- 564 54. Dobin A, Davis CA, Schlesinger F, Drenkow J, Zaleski C, Jha S, et al. STAR: ultrafast universal RNA-
565 seq aligner. *Bioinformatics*. 2013;29:15–21. doi:10.1093/bioinformatics/bts635.
- 566 55. Forstner KU, Vogel J, Sharma CM. READemption--a tool for the computational analysis of deep-
567 sequencing-based transcriptome data. *Bioinformatics*. 2014;30:3421–3.
568 doi:10.1093/bioinformatics/btu533.
- 569 56. Rozanski A, Moon H, Brandl H, Martín-Durán JM, Grohme MA, Hüttner K, et al. PlanMine 3.0-
570 improvements to a mineable resource of flatworm biology and biodiversity. *Nucleic Acids Res*.
571 2019;47:D812–20. doi:10.1093/nar/gky1070.
- 572 57. Al-Ghalith, Knights G, Knights D. BURST enables optimal exhaustive DNA alignment for big data.
573 2017. doi.org/10.5281/zenodo.806850.
- 574

Figure 1

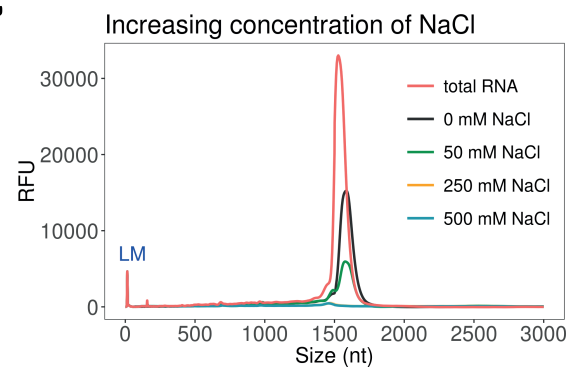
A



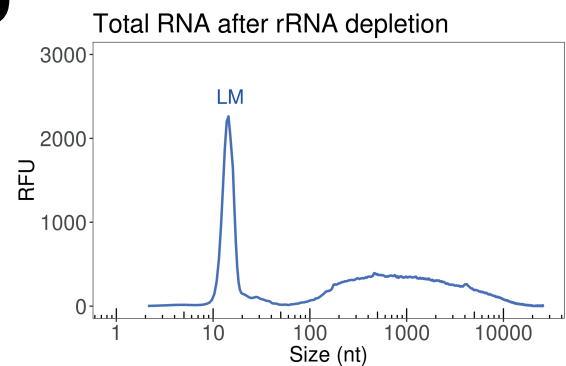
B



C



D



E

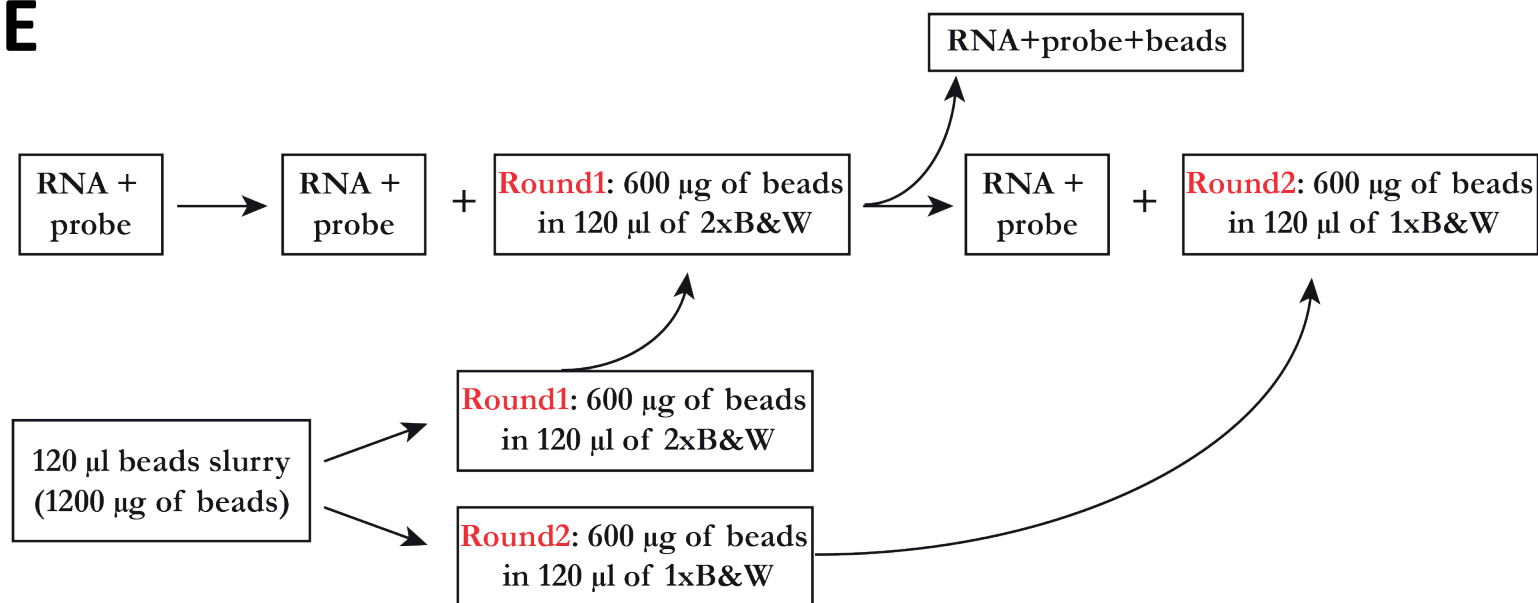


Figure 1. Efficiency of rRNA removal from total planarian RNA.

(A) Schematic representation of rRNA depletion workflow. Biotinylated DNA probes are hybridized to rRNA, followed by subtraction of rRNA-DNA hybrids using streptavidin-labeled magnetic beads.

(B) Separation profile of planarian total RNA. The large peak at 1527 nts corresponds to the co-migrating 18S rRNAs and the two fragments of processed 28S rRNA. LM stands for lower marker with the length of 15 nt

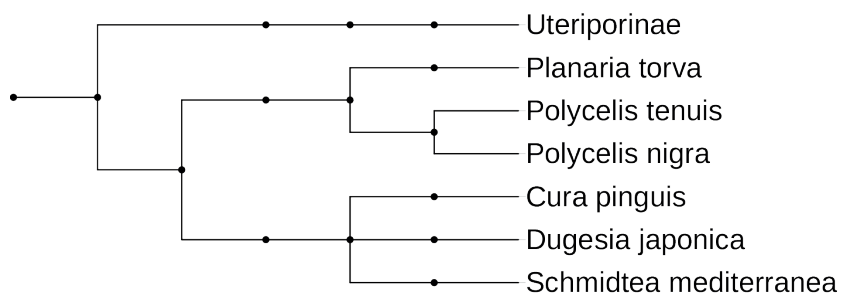
(C) Increasing concentration of NaCl improves the efficiency of rRNA removal.

(D) Total planarian RNA after rRNA depletion.

(E) Removal of rRNA-DNA hybrids was performed in two consecutive steps using streptavidin-coated magnetic beads resuspended in 2x of 1x B&W buffer.

Figure 2

A



B

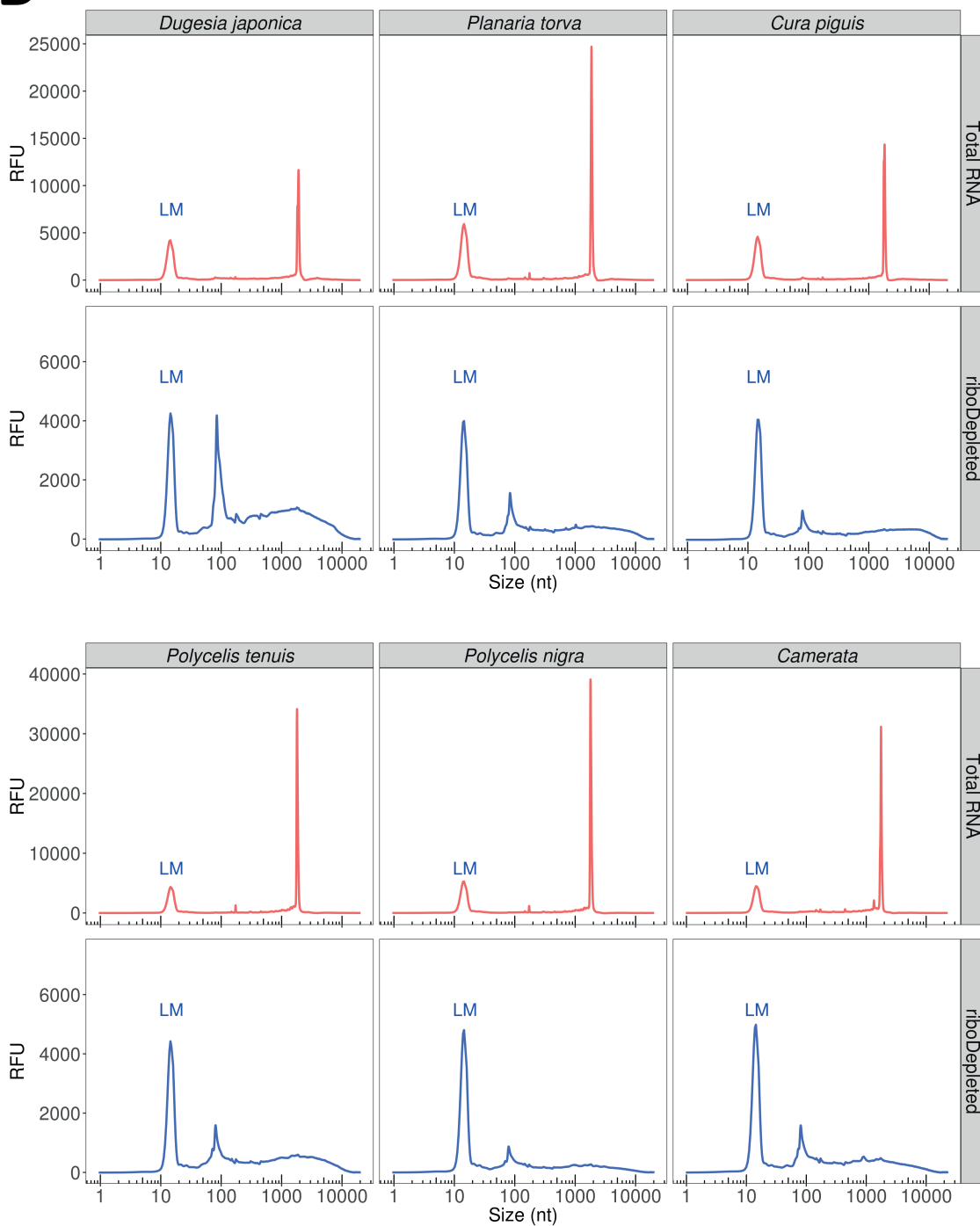


Figure 2. Probes developed for *S. mediterranea* efficiently remove rRNA of other freshwater triclads

(A) Phylogenetic tree showing the taxonomic position of the analyzed planarian species. **(B)** Separation profile of total RNA before and after rRNA depletion. In all species analyzed the 28S rRNA undergoes the “gap deletion” maturation that result in two co-migrating fragments. Both 28S fragments co-migrate with 18S rRNA, resulting in a single rRNA peak. The peak at about 100 nts represents a variety of small RNAs (5S and 5.8S rRNA, tRNAs, and other small RNA fragments) that evaded size selection by the RNA Clean & Concentrator-5 kit (Zymo Research).

Figure 3

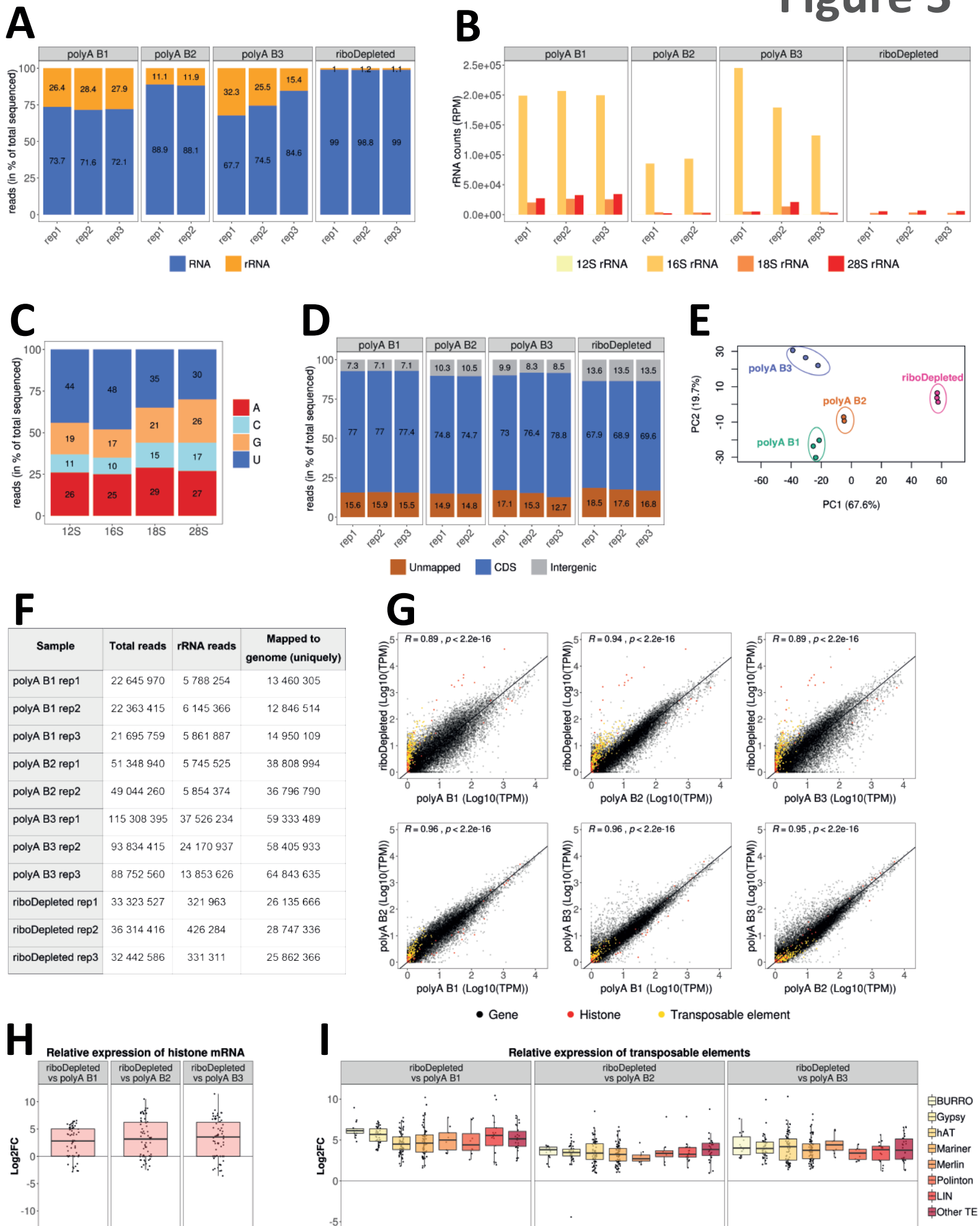


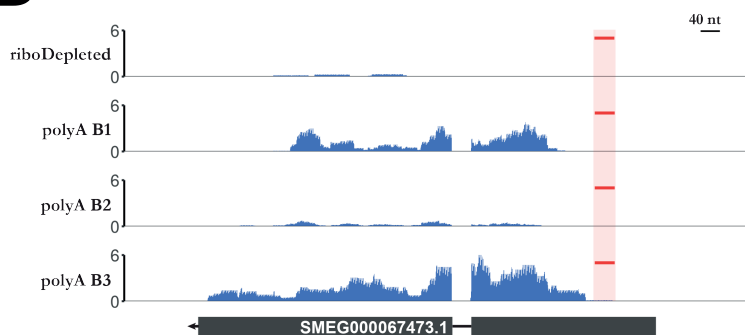
Figure 3. Comparison of rRNA-depleted and poly(A)-enriched planarian RNA-Seq libraries.

(A) Percentage of rRNAs reads in the sequenced libraries prepared from rRNA-depleted or poly(A)-enriched RNA. **(B)** Species of rRNAs remaining in the final sequenced libraries. **(C)** Nucleotide content of planarian rRNA. **(D)** Percentage of sequenced reads mapped to coding (CDS) and intergenic regions in the planarian genome. **(E)** Principal component analysis (PCA) biplot of log₂ expression data for coding genes reveals distinct clustering of all analyzed RNA-Seq experiments. **(F)** Sequencing depth and number of reads mapped to the planarian genome in analyzed rRNA-depleted and poly(A)-enriched samples. **(G)** Comparison of gene expression in transcripts per million (TPM) between planarian ribodepleted and poly(A)-enriched (polyA) RNA-Seq data. The Pearson's correlation coefficient is indicated. **(H)** Increased representation of histone mRNAs in ribodepleted libraries. **(I)** Boxplot of log₂ fold changes of the expression of transposable elements between ribodepleted and poly(A)-enriched libraries.

A

Gene_id	TPM in polyA B1	TPM in polyA B2	TPM in polyA B3	TPM in ridoDepleted	LFC polyA+ B1	LFC polyA+ B2	LFC polyA+ B3	Annotation
SMESG000014330.1	0.27	0.24	0.38	0.005	-5,82	-5,30	-6,41	rhodopsin-like orphan gpcr
SMESG000068163.1	0.38	0.15	0.08	0.006	-6,13	-4,39	-3,89	NA
SMESG000069530.1	0.26	0.102	0.027	0.006	-5.99	-4.34	-2.51	NA
SMESG000022863.1	10.05	2.78	10.47	0.60	-4.23	FALSE	-4.34	NA
SMESG000021061.1	10.94	10.32	15.38	5.38	-1.27	-0.82	-1.77	MS3_11207 (MYDGF)
SMESG000067473.1	17.62	6.69	20.57	1.13	-4.21	-2.44	-4.45	MS3_08805 (GID8)
SMESG000044545.1	30.91	32.22	34.31	16.72	-1.11	-0.82	-1.25	REEP2
SMESG000043656.1	48.2	24.8	36.5	12.3	-2,20	-0,88	-1,81	COX11
SMESG000066644.1	1020.6	605.8	798.9	51.9	-4,53	-3,41	-4,19	RPL26

B



C

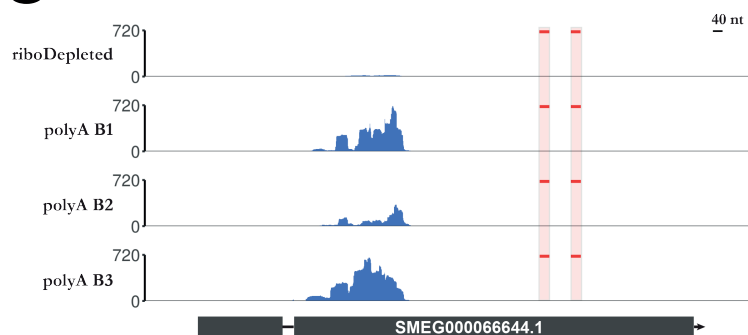
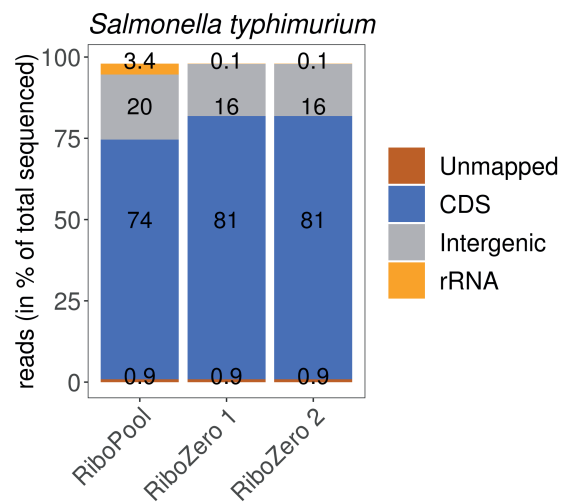


Figure 4. Off-target analysis of DNA probes used for rRNA depletion

(A) Expression level of nine transcripts targeted by designed probes. **(B)** RNA-Seq coverage profile for SMESG000067473.1 in rRNA depleted (ribodepleted) and poly(A) enriched (polyA B1, polyA B2, polyA B3) libraries. The position of antisense probes mapping to the transcripts is marked in red. **(C)** The same as (B) for SMESG000066644.1.

A



B

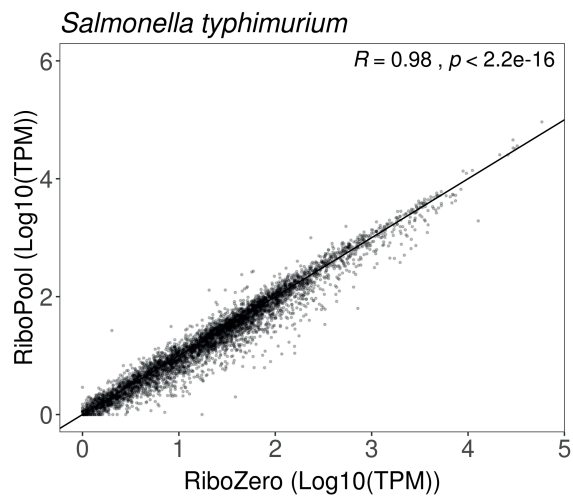
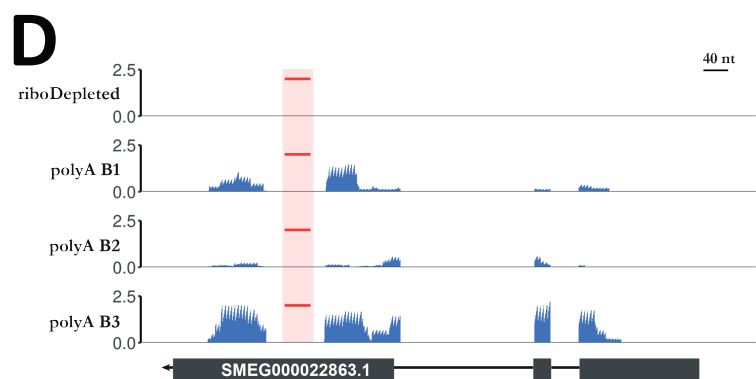
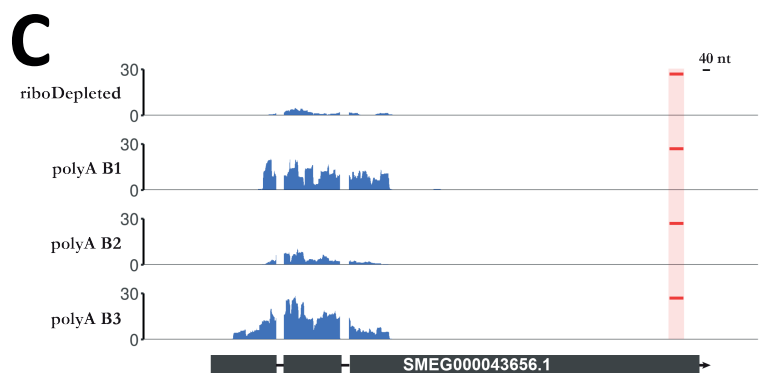
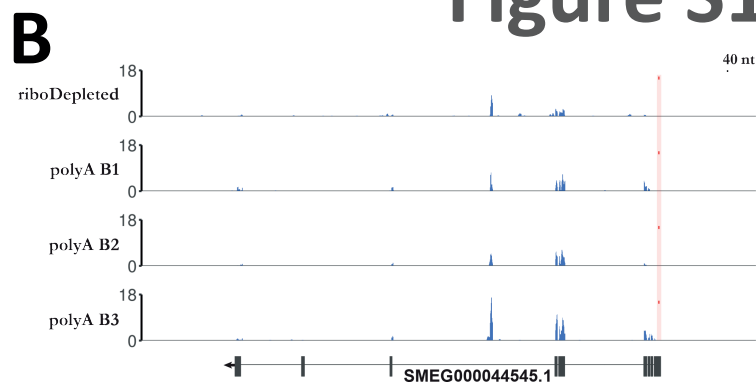
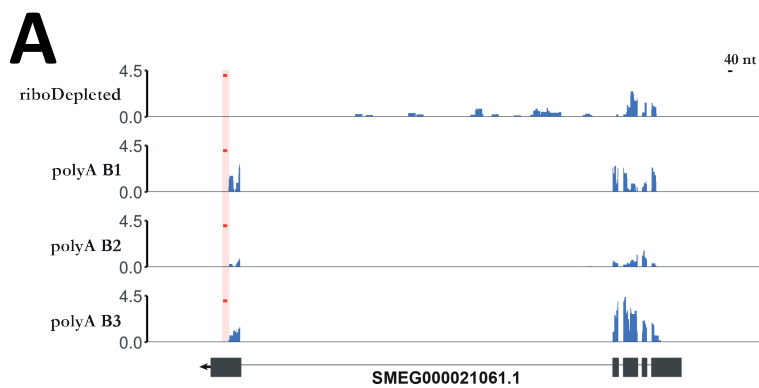


Figure 5. Application of the developed rRNA workflow to other species using organism-specific probes.

(A) Percentage of rRNAs in *Salmonella typhimurium* sequenced libraries prepared using our developed rRNA depletion workflow with organism-specific RiboPool probes or the commercial Ribo-Zero kit. **(B)** Scatter plot showing the transcript abundance (transcript per million (TPM)) between rRNA depleted libraries using our developed workflow or the Ribo-Zero commercial kit. The Pearson's correlation coefficient is indicated.

Figure S1



Supplemental Figure S1.

(A)-(D) RNA-Seq coverage profile for genes potentially targeted by designed probes in rRNA depleted (ribodepleted) and poly(A) enriched (polyA B1, polyA B2, polyA B3) libraries. The position of antisense probes mapping to the transcripts is marked in red.